

# Polyelectrolyte-assisted soft reduced process for Pt-Cu nanoclusters with enhanced electrocatalytic activity for the methanol oxidation reaction

Rui Li<sup>a</sup>, Shengnan Li<sup>a</sup>, Yong Liu<sup>a</sup>, Tsuyoshi Ochiai<sup>b,c</sup>, Sanjay S. Latthe<sup>a,b</sup>, Kazuya Nakata<sup>b</sup>, Ruimin Xing<sup>a,b,\*\*</sup>, Shanhu Liu<sup>a,b,\*</sup>

<sup>a</sup> Henan Key Laboratory of Polyoxometalate Chemistry, Henan Joint International Research Laboratory of Environmental Pollution Control Materials, College of Chemistry and Chemical Engineering, Henan University, Kaifeng, PR China

<sup>b</sup> Research Institute for Science and Technology, Photocatalysis International Research Center, Tokyo University of Science, 2641 Yamazaki, Noda, Chiba, 278-8510, Japan

<sup>c</sup> Local Independent Administrative Agency, Kanagawa Institute of Industrial Science and Technology (KISTEC), Kanagawa, 213-0012, Japan

## ARTICLE INFO

### Keywords:

Methanol oxidation reaction  
Nanocrystal clusters  
Electrocatalysts  
Pt-Cu bimetallic alloy

## ABSTRACT

Noble metal-based bimetallic alloy nanostructures became popular for methanol oxidation reaction (MOR) in order to lower the high cost of the Pt catalyst and improve the catalyst activity as well as their CO tolerance. Fabrication of the secondary structures of bimetallic alloy nanocrystal clusters is desired due to their abundant accessible active sites and enhanced stability. Herein, for the first time, we prepared novel Pt-Cu bimetallic alloy nanocrystal clusters (Pt-Cu BANCs) in the presence of poly(diallyldimethylammonium chloride) (PDDA). The selective use of PDDA and control of the amount of PDDA are critical to the controlled fabrication of secondary structures with nanograins assembled together. The Pt-Cu BANCs offered abundant active sites available and enhanced durable stability, and are investigated to be high-performance electrocatalysts for MOR (i.e. the ECSAs of Pt-Cu BANCs and the specific current density of methanol oxidation on Pt-Cu BANCs are 73.9 m<sup>2</sup>/g and 3.36 mA·cm<sup>-2</sup>, respectively), which are far better than those of commercial Pt/C and Pt black. Our results reported herein developed an effective strategy of polyelectrolyte-assisted soft reduced process for the creation of the secondary structures of bimetallic alloy nanocrystal clusters, which would be used as enhanced catalysts in the field of clean energy.

## 1. Introduction

Direct methanol fuel cells (DMFCs) as a viable and portable energy conversion device hold great potential among advanced energy conversion technologies due to their low power density but high energy density [1–3]. Active and durable electrocatalysts for methanol oxidation reaction (MOR) are of critical importance to the commercial viability of DMFC technology. Pt-based catalysts remain as the most active catalysts for use due to the dissociative adsorption of methanol in strong acidic media [4–9]. Unfortunately, besides the high cost and the rare reserves, Pt-based catalysts are susceptible to the poisoning effect of CO usually produced during the methanol decomposition process, which heavily hindered the commercialization of DMFC technology. To address these issues, Pt-based bi-/multi-metallic alloys and Pt ternary

catalysts (Pt integrated with other 3d-transition metals) have received much interest due to the enhanced catalytic activity and CO tolerance as well as the cost reduction [10–20].

Size and structure control is an effective strategy for tuning the physical and chemical properties of metal alloy nanocrystals and thus their catalytic activity [21–25]. Up to now, various Pt-Cu bimetallic alloys with different morphological features have been prepared for MOR, including nanowires [5,22], nanocubes [26,27], nanoframes [28–30], nanoparticles [7,13,31–34], nanocages [35], nanodendrites [6,7,36] and various polyhedrons [37], mostly by using a template, seed-mediated method or galvanic displacement reaction that required multi-step or complicated synthetic procedures and/or the use of organic solvents. Comparatively, the synthesis of metal alloy hierarchical architectures by a facile method remains rare [12]. Fabrication of the

\* Corresponding author. Henan Key Laboratory of Polyoxometalate Chemistry, Henan Joint International Research Laboratory of environmental pollution control materials, College of Chemistry and Chemical Engineering, Henan University, Kaifeng, PR China.

\*\* Corresponding author. Henan Key Laboratory of Polyoxometalate Chemistry, Henan Joint International Research Laboratory of environmental pollution control materials, College of Chemistry and Chemical Engineering, Henan University, Kaifeng, PR China.

E-mail addresses: [rmxing@henu.edu.cn](mailto:rmxing@henu.edu.cn) (R. Xing), [liushanhu@vip.henu.edu.cn](mailto:liushanhu@vip.henu.edu.cn) (S. Liu).

<https://doi.org/10.1016/j.jpcs.2018.10.002>

Received 25 June 2018; Received in revised form 30 September 2018; Accepted 2 October 2018

Available online 02 October 2018

0022-3697/ © 2018 Elsevier Ltd. All rights reserved.

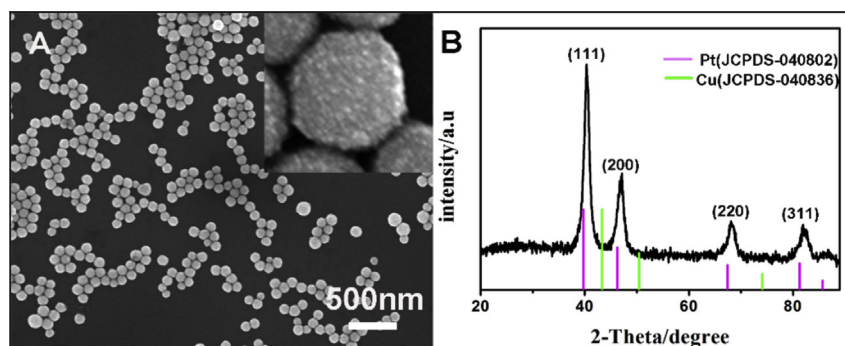


Fig. 1. SEM image (A) and XRD patterns (B) of Pt-Cu BANCs. The inset in (A) is a high-resolution SEM image of Pt-Cu BANCs.

secondary structures of bimetallic alloy nanocrystal clusters is specially desired due to their abundant accessible active sites and enhanced stability, which offers a flexible means to associate the size-dependent electrocatalytic properties of nanocrystals with the possibility to tune the collective properties (e.g. durable stability) due to their interconnected structures. Herein, for the first time, we introduced a poly-electrolyte-assisted soft reduced process for the synthesis of Pt-Cu BANCs via a one-pot procedure. The electrocatalytic activity and stability of the Pt-Cu BANCs towards MOR was evaluated in comparison with that of commercial Pt/C and Pt black.

## 2. Experimental section

### 2.1. Chemicals

Poly (diallyldimethylammonium chloride) (PDDA, 20 wt %) were bought from Sigma. Hexachloroplatinic (IV) acid hexahydrate ( $\text{H}_2\text{PtCl}_6 \cdot 6\text{H}_2\text{O}$ ) was purchased from Sinopharm Chemical Reagent Co. Ltd, (Beijing, China). Copper (II) chloride dihydrate ( $\text{CuCl}_2 \cdot 2\text{H}_2\text{O}$ ) was obtained from Tianjin Fengchuan Chemical Reagent Co. Ltd. All reagents were used as received without further purification.

### 2.2. Synthesis of Pt-Cu BANCs catalyst

In a typical synthesis, 4 mL of  $\text{H}_2\text{PtCl}_6 \cdot 6\text{H}_2\text{O}$  (20 mM), 4 mL of  $\text{CuCl}_2 \cdot 2\text{H}_2\text{O}$  (20 mM) was dissolved in 16 mL of the PDDA solution. After 30 min of stirring, the solution was transferred to a 25 mL Teflon-lined stainless steel autoclave. The autoclave was heated at 200 °C for 1 h and then allowed to cool to room temperature. The sample collected by centrifugation was washed with ethanol and deionized water several times to remove impurities. Finally, the catalyst was dispersed in ethanol solution for further characterization.

### 2.3. Characterization

Energy dispersive X-ray (EDX) analysis and scanning electron microscopic (SEM) pictures and were performed using a JSM-7610F scanning electron microscope (Hitachi). Selected area electron diffraction (SAED) patterns and transmission electron microscopy (TEM) pictures and were completed using a JEOL JEM-2100 transmission electron microscope. X-ray diffraction (XRD) patterns were obtained on an X-ray D8 Advance instrument (Bruker, Germany). X-ray photoelectron spectroscopy (XPS) was completed using Thermo Scientific Escalab 250Xi.

### 2.4. Electrochemical measurements

Electrochemical measurements such as amperometric and cyclic voltammetry (CV) measurement were accomplished using a standard three-electrode cell with a CHI 660D electrochemical workstation

(Chenhua, Shanghai) at 20 °C. A modified glassy carbon electrode acted as the work electrode, with a Pt wire and AgCl/Ag electrode saturated as the counter electrode and reference electrode. The working electrode ( $d = 3.0$  mm) was a glassy carbon disk polished with  $\text{Al}_2\text{O}_3$  paste, and washed thoroughly with deionized water and nitric acid solution. Five milligrams of the catalysts powder were ultrasonically dispersed in 0.5 mL  $\text{CH}_3\text{OH} + 0.5$  mL  $\text{H}_2\text{O}$  for 1 h to ensure the catalysts uniformly dissolving in the solution. Five microliters of the nanocatalyst suspension (5 mg/mL) was released onto the work electrode. After being dried for in an incubator 30 min, the dried catalyst layer on the top of the electrode was covered with 5  $\mu\text{L}$  of the Nafion alcohol solution (0.1 wt %) and then dried. The working electrodes were first activated in 0.5 M  $\text{H}_2\text{SO}_4$  solution until a steady CV was obtained ( $-0.2$ – $1.0$  V at 50 mV/s). Then, the methanol electro-oxidation measurements were conducted in 0.5 M  $\text{H}_2\text{SO}_4$  solution with 1M  $\text{CH}_3\text{OH}$ . For the commercial Pt/C or Pt black catalysts (Alfa Aesar), the same procedure was carried out with 5 mg/mL of the concentration of the catalyst inks.

## 3. Results and discussion

### 3.1. Structural and compositional investigation

The preparation of Pt-Cu BANCs was very simple, only with the co-reduction of noble metal precursors ( $\text{H}_2\text{PtCl}_6$  and  $\text{CuCl}_2$ ) in the presence of PDDA at 200 °C for 1 h via a one-pot procedure. PDDA, a positively charged polyelectrolyte with repeated quaternary ammonium centers, has modest reducibility, excellent hydrophilic properties and high chemical stability, and herein, served as soft reductant and stabilizing agent for the synthesis of Pt-Cu BANCs for the first time.

The conformation and size dispersal of the product were explored by SEM analyses. As Fig. 1A shows, the product exhibits an apparent and uniform spherical morphology with a monodispersed particles on a big scale. Statistical analyses indicate that the spherical particles have an average diameter of 107 nm with a relatively narrow size distribution (ESI, Fig. S1). The HR-SEM image (Inset of Fig. 1A) presents that the nanospheres be made up of many primary nanograins assembled together and therefore have the secondary structural characteristic of nanocrystal clusters. Its EDX spectra (ESI, Fig. S2) in the typical procedure indicates the corresponding atomic ratio of Pt to Cu was approx 10: 1, not in accordance with the initial dosage. The related elemental mapping reveals the highly uniform dispersion of element Pt and Cu into the nanocrystal clusters (ESI, Fig. S3). In addition, the XRD patterns (Fig. 1B) further indicate the alloy structures of the clusters, in which all the diffraction peaks are positioned between fcc Cu (JCPDS: 04–0836) crystal phases and face centered cubic (fcc) Pt (JCPDS: 04–0802), with no other diffraction peaks from either pure Cu or pure Pt being identified. Using the Debye-Scherrer formula calculations for the strongest peak (111) in XRD patterns showed the crystal size of about 5.5 nm. This result fully suggests the formation of secondary structures with nanograins assembled together, in accordance with the

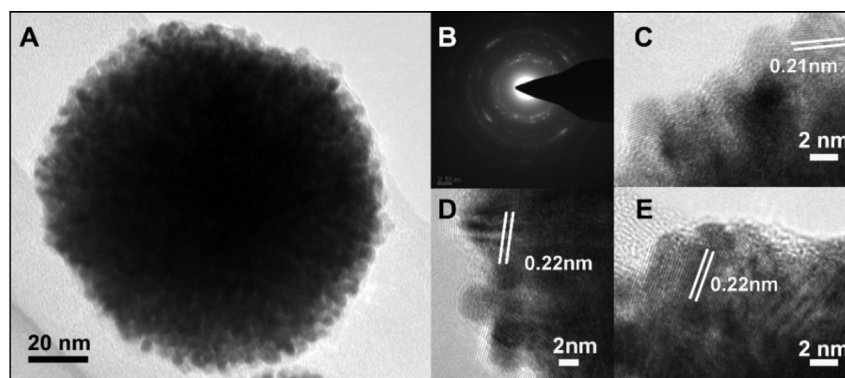


Fig. 2. Low resolution TEM image (A), the corresponding SAED patterns (B) and high-resolution TEM images (C, D and E) of Pt-Cu BANCs.

SEM observations, which offered abundant active sites available and enhanced stability, as suggested by our previous reports [38,39].

Detailed structural information of the alloy structure was more studied by TEM analyses. As TEM image demonstrated that in Fig. 2A, the nanocrystals aggregated to generate a spherical three-dimensional hierarchical cluster. The SAED pattern (Fig. 2B) gained from a single nanosphere suggests that the cluster has polycrystalline-like diffraction profiles. A passes inspection by HRTEM images (Fig. 2C–E) demonstrates that these primary grains (4 nm - 6 nm) display high crystallinity and accumulate accidentally to procedure the cluster nanostructure. Clear crystal lattice fringes with the spacings of 0.22 nm and 0.21 nm are witnessed, which are reliable with the values for the (111) crystal planes of Pt-Cu bimetallic alloy. It is reported that the (111)-oriented crystallization is exceptionally beneficial to the enhancement of the catalytic reactivity of Pt-Cu alloy [40].

Since the electrocatalytic process of the MOR only occurs on the electrode surface, XPS as a surface sensitive technique, was employed to investigate the composition and valence state on the surface of Pt-Cu BANCs. As Fig. 3A shows, the Cu 2p spectrum exhibits the two peaks at 931.8 eV ( $2p_{3/2}$ ) and 951.7 eV ( $2p_{1/2}$ ), suggestive of elemental  $\text{Cu}^0$ . The presence of  $\text{Cu}^0$  helps improve anti-CO ability and show a better stability in process of methanol oxidation reaction. Whereas two Pt 4f peaks situated at 74.38 eV and 71.08 eV could be attributed to the Pt  $4f_{5/2}$  and Pt  $4f_{7/2}$  of metallic  $\text{Pt}^0$  and the percentage of  $\text{Pt}^0$  species is 81.1% (Fig. 3B). In addition, the weaker doublet at 75.5 eV and 72.5 eV could be attributed to  $\text{Pt}^{\text{II}}$  in the oxidized forms on the surface of the sample. Meanwhile, compared to that of commercial Pt black as previously reported, the Pt 4f binding energy in the Pt-Cu BANCs negatively shifted 0.51 eV [36]. The negative shift of the Pt 4f peaks showed the obvious change in the Pt electronic structure, primarily originating from the electron donation from Cu elements to Pt elements due to the different electro-negativity and thus further confirming the formation of Pt-Cu alloy. The varied electronic consequence may result in the

optimization of binding energy of the reactive species involved in MOR on the surface of the catalysts, thus improved the catalytic electro-activity of Pt [8,36,41].

To better recognize the formation mechanism of Pt-Cu BANCs and the role of the soft reductant of PDDA, two kinds of regulate experiments were approved of as follows. Control A was to vary the amount of PDDA. Control B was to add NaI as an additional reductant into the typical experiment. Each control experiment was completed in the same situations and procedure as the typical experiments.

In the control A experiment, when the amount of PDDA is 2 mL, the products were bigger three-dimensional hierarchical structures which were form of larger building blocks instead of primary nanograins (Fig. 4A). Increasing PDDA resulted in the decreased dimensions of the hierarchical structures accompanying with decreased primary nanograins (Fig. 4B and C). But too much PDDA led to the getatiniform and inhomogeneity of the product (Fig. 4D). This is because excessive PDDA would slow down the dissociation rate of metal complexes (formed by positive PDDA molecules and  $\text{PtCl}_6^{2-}$ ), which affect the nucleation process and the interface microenvironment of primary nanograins. Therefore, the suitable amount of PDDA was critical for the synthesis of well-dispersed and uniform Pt-Cu BANCs consisting of tiny primary nanograins.

In control B experiment, NaI was added as an additional reductant, which was regarded to influence the surface shape of metals by etching process [12,42]. When adding 80 mg of NaI into the typical experiment, the product is urchin-like hierarchical structure with an average dimension of 1.2  $\mu\text{m}$ , which were form of larger sphere instead of primary nanograins (ESI, Fig. S4A). Its EDX pattern (ESI, Fig. S4B) and the element mapping profiles (ESI, Fig. S4C) demonstrated the regular distribution of Cu and Pt in the urchin-like Pt-Cu nanostructures (Pt-Cu NSs). Its XRD pattern (ESI, Fig. S4D) further illustrated the formation of Pt-Cu alloy. Therefore, NaI as reductant and etchant, was presumed to accelerate the formation of Pt and Cu crystal nuclei and affect the

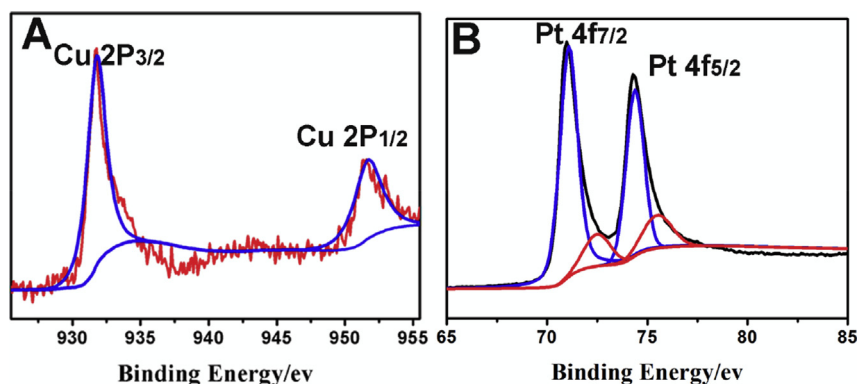
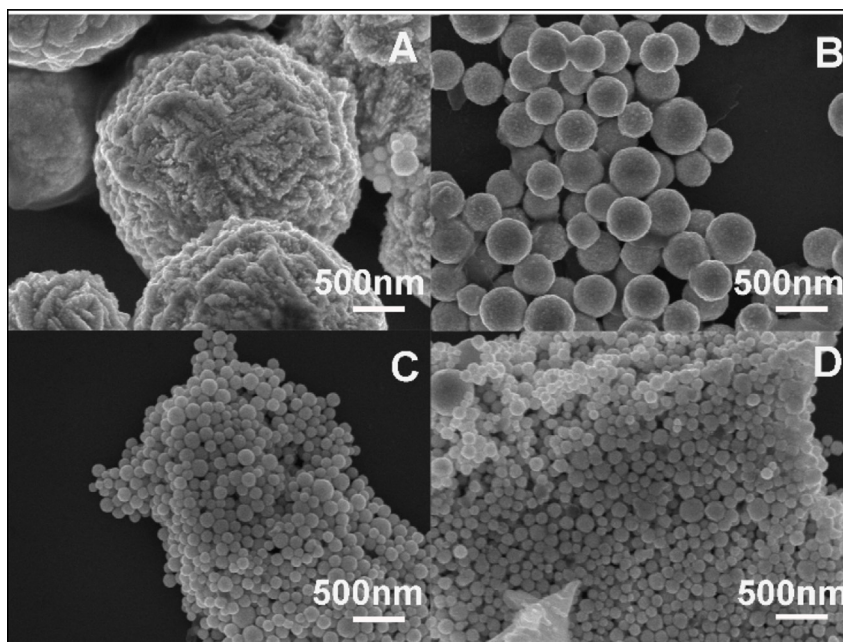


Fig. 3. XPS spectra of Pt-Cu BANCs in Cu 2p (A) and Pt 4f (B) regions.



**Fig. 4.** SEM images of different amounts of PDDA in the synthesis of Pt-Cu BANCs: 2 ml PDDA + 14 ml H<sub>2</sub>O (A), 8 ml PDDA + 8 ml H<sub>2</sub>O (B), 24 ml PDDA (C), 32 ml PDDA (D).

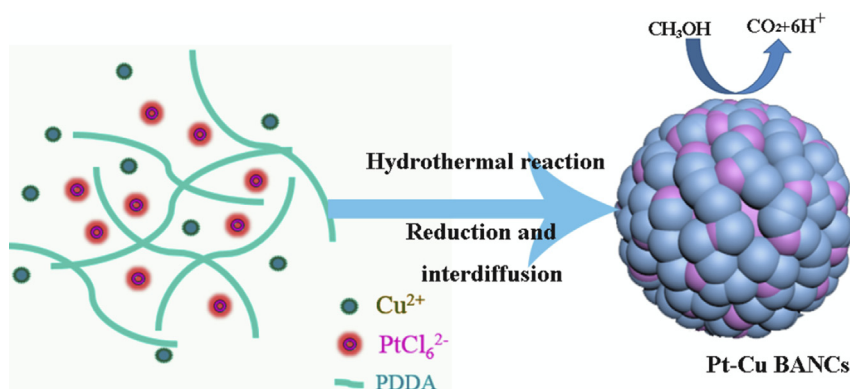
surface shape of alloy metals by etching process.

The formation mechanism of Pt-Cu BANCs was illustrated in [Scheme 1](#). PDDA, a positively charged polyelectrolyte with repeated quaternary ammonium centers, has modest reducibility, excellent hydrophilic properties and high chemical stability. Herein it was presumed as reductant and stabilizing agent to ensure the formation of isolated Pt crystal nuclei, possibly via the electrostatic interaction between positive PDDA molecules and PtCl<sub>6</sub><sup>2-</sup>; and then the preformed Pt crystal nuclei may make the reduction of Cu<sup>II</sup> precursor to Cu<sup>0</sup> crystal nuclei happen via the autocatalytic growth mechanism [36]. The deposited Cu atoms mixed with Pt atoms via an interdiffusion process to form the alloy nanograins because of thermal energy [36]. These primary nanograins and PDDA molecules spontaneously aggregated into a spherical secondary structure, nanocrystal clusters, to realize the minimization of their surface energy. Advance hydrothermal treatment bring about the growth of Pt-Cu BANCs in the Ostwald ripening process, leaving behind Pt-Cu BANCs with different dimensions and sizes. In contrast to other methodologies, PDDA was employed as a soft reductant for the synthesis of Pt-Cu BANCs in this work, which greatly simplified the synthetic procedures for the Pt-Cu alloy and promote their structural controllability.

### 3.2. Electrocatalytic performance

The MOR was chosen as a typical reaction for estimating the electrocatalytic performance of the as-prepared Pt-Cu nanostructures. Commercial Pt/C and Pt black (Alfa Aesar) were compared under the same conditions. The electrochemically active surface area (ECSA) reveal that the amount of available active sites on Pt-Cu alloy, which can be dictated from the electric charges of hydrogen adsorption and desorption by CV in 0.5 M H<sub>2</sub>SO<sub>4</sub>. As [Fig. 5A](#) shows, the ECSAs of Pt-Cu BANCs, Pt-Cu NSs, commercial Pt/C and Pt black are 73.9, 6.5, 57.1 and 37.3 m<sup>2</sup>/g, respectively. This outcome evidently demonstrated that Pt-Cu BANCs are electrochemically more available, benefiting from the nanocrystal cluster structure with many primary nanograins. Whereas the lower ECSA of Pt-Cu NSs is ascribed to the urchin-like hierarchical structure with bigger dimensions which were composed of larger building blocks [35].

As [Fig. 5B](#) shows, two obvious anodic peaks are observed on these catalysts, which are typical features of MOR with intermediate carbonaceous species oxidation peak at lower potential and methanol oxidation peak at higher potential during the positive and negative scan directions [36]. The specific current density (*J*) was standardized to the ECSA of the electro-catalysts and accustomed to estimation the actual value of the essential activity of the electrocatalysts. The specific



**Scheme 1.** Schematic illustration of Pt-Cu BANCs synthesis.

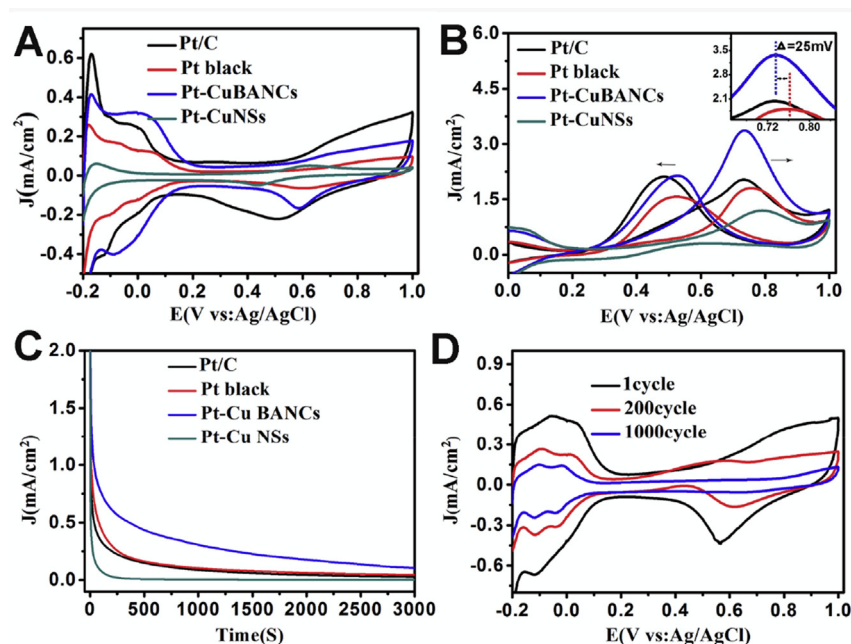


Fig. 5. Comparison of electrocatalytic performance of Pt-Cu BANCs, Pt-Cu NSs, commercial Pt/C and Pt black. (A) CVs in N<sub>2</sub>-saturated 0.5 M H<sub>2</sub>SO<sub>4</sub>, (B) specific activities in N<sub>2</sub>-saturated 0.5 M H<sub>2</sub>SO<sub>4</sub> + 1 M CH<sub>3</sub>OH, and (C) chronoamperometric curves in 0.5 M H<sub>2</sub>SO<sub>4</sub> + 1 M CH<sub>3</sub>OH at 0.72 V; (D) CVs on Pt-Cu BANCs after 1000 cycles in 0.5 M H<sub>2</sub>SO<sub>4</sub> solution. The scan rate is 50 mV/s.

current density of methanol oxidation on Pt-Cu BANCs (3.36 mA/cm<sup>2</sup>) is 1.65 times higher than that on Pt/C (2.03 mA/cm<sup>2</sup>), and 1.86 times higher than that of Pt black (1.8 mA/cm<sup>2</sup>) (ESI, Fig. S5), suggesting that Pt-Cu BANCs have a large improvement in electrocatalytic activity. Meanwhile, methanol oxidation peak current on Pt-Cu BANCs is also higher than those of hollow Pt-Cu catalyst (2.08 mA/cm<sup>2</sup>), Pd<sub>50</sub>Pt<sub>50</sub> (1.08 mA/cm<sup>2</sup>) [43], dendritic PtNi NCs (1.76 mA/cm<sup>2</sup>) and flower-like PtNi NCs (0.8 mA/cm<sup>2</sup>) [44], PtCu<sub>3</sub> alloy hexapods (2.96 mA/cm<sup>2</sup>) [28], Pt-Ni DLNBs (1.06 mA/cm<sup>2</sup>) [45] and ROH Pt-Ni-Cu NCs (2.61 mA/cm<sup>2</sup>) [19] which further indicates that Pt-Cu BANCs show competitive electrocatalytic activity for the MOR. Compared to Pt black, the oxidation peak potential of methanol on Pt-Cu BANCs negatively move *ca.* 25 mV, further indicating enhanced electrocatalytic activity at low potential. During the MOR process, Pt electrocatalysts was easily inactivated by the adsorption of carbonaceous species (such as CO<sub>ads</sub> and non-CO<sub>ads</sub> species). The ratio of  $I_f/I_b$  (where  $I_b$  and  $I_f$  are the reverse current peak and the forward oxidation current peak) is a key parameter to estimate the poison tolerance of the electrocatalysts to the carbonaceous species during the MOR. A higher number of  $I_f/I_b$  shows more efficient oxidization of methanol and less produce of poisoning species on the electrocatalyst surface [10]. The  $I_f/I_b$  ratio of Pt-Cu BANCs (1.57) was higher than that of commercial Pt/C (0.96) and Pt black (1.14), indicating that the recombination of Cu in Pt-based catalysts indeed enhance the CO tolerance.

The electrocatalytic stability of those catalysts for MOR were investigated by chronoamperometry. As Fig. 5C shows, in the course of the whole reaction route, the methanol oxidation current on Pt-Cu BANCs was always higher than that on the other three catalysts (Pt-Cu NSs, commercial Pt/C and Pt black). Besides, the durability of Pt-Cu BANCs was studied through the CV cycling treatment performed in 1 M CH<sub>3</sub>OH + 0.5 M H<sub>2</sub>SO<sub>4</sub> solution. After 200 cycles, Pt-Cu BANCs retained 70% of their initial value, however the Pt/C catalyst dropped to 66.1% of its early value in the equal testing situations (ESI, Fig. S6). After 1000 cycles, the ECSA of the Pt-Cu BANCs decreased from 73.9 m<sup>2</sup>/g to 25.1 m<sup>2</sup>/g (Fig. 5D), slightly below the initial ECSA of Pt black (37.3 m<sup>2</sup>/g). The above results suggest the enhanced electrocatalytic activity and stability of Pt-Cu BANCs as an electro-catalyst for MOR compared to the commercial Pt-based catalysts. It is reported that the decrease of the electrocatalytic activity mainly result from CO poisoning and the sample agglomeration/migration during the MOR. Obviously, the high CO tolerance of Pt-Cu BANCs is responsible for the

enhanced stability.

Based on the above discussion, the enhanced electrocatalytic activity and stability of Pt-Cu BANCs as well as the improved CO tolerance could be attributed to the two following factors: 1) the secondary structures of Pt-Cu BANCs consisting of many primary nanograins assembled together, which not only supplied abundant active sites for MOR, but also exhibited durable stability due to the larger secondary structures compared with monodispersed nanocrystals; 2) the synergistic effects between Cu and Pt atoms due to the bimetallic alloy feature, that is, the incorporation of Cu in Pt-based catalysts could dilute/insulate the adjacent Pt atoms on the surface because of the geometric effect and also could contribute electron density to the d-bands of Pt because of the electronic result, which thus altered the adsorption orientation and influenced the adsorption energies of reactants and reaction products. More specifically, the Cu molecules close the surface of the compound Pt nanoparticles could support the adsorption of oxygen species for example OH<sub>ads</sub>, which accelerated the oxidation of CO in process material and therefore led to the higher electrocatalytic activity on the way to MOR [46,47].

#### 4. Conclusions

In summary, Pt-Cu BANCs have been synthesized by a facile poly-electrolyte-assisted soft reduced process. PDDA was presumed as reductant and stabilizing agent to ensure the formation of isolated Pt crystal nuclei. Electrochemical measurements reveal that Pt-Cu BANCs show enhanced MOR activity and long-term durability as well as the improved CO tolerance, compared to commercial Pt black and Pt/C. Taking into consideration the secondary structures of Pt-Cu BANCs consisting of many primary nanograins assembled together, the enhanced electrocatalytic activity of Pt-Cu BANCs were presumably attributed to their abundant accessible active sites due to the secondary structures consisting of ultrafine primary nanograins, and the synergistic effects between Pt and Cu atoms due to the bimetallic alloy feature (i.e. geometric effect and electronic effect). Our results reported herein developed an effective strategy for the creation of the secondary bimetallic alloy nanocrystal clusters, which could be used as high-performance catalysts in the field of clean energy.

## Acknowledgments

We greatly appreciate the support of the Foundation of Henan Educational Committee (17A150023), Key Technology Research Foundation of Henan Province (172102410078, 172102310532).

## Appendix A. Supplementary data

Supplementary data to this article can be found online at <https://doi.org/10.1016/j.jpccs.2018.10.002>.

## References

- N. Kakati, J. Maiti, S.H. Lee, S.H. Jee, B. Viswanathan, Y.S. Yoon, Anode catalysts for direct methanol fuel cells in acidic media: do we have any alternative for Pt or Pt-Ru? *Chem. Rev.* 114 (2014) 12397–12429.
- J. Zhang, K. Li, B. Zhang, Synthesis of dendritic Pt-Ni-P alloy nanoparticles with enhanced electrocatalytic properties, *Chem. Commun.* 51 (2015) 12012–12015.
- L.-Y. Jiang, X.-Y. Huang, A.-J. Wang, X.-S. Li, J. Yuan, J.-J. Feng, Facile solvothermal synthesis of Pt<sub>76</sub>Co<sub>24</sub> nanomyriapods for efficient electrocatalysis, *J. Mater. Chem.* 5 (2017) 10554–10560.
- M.-T. Liu, L.-X. Chen, A.-J. Wang, K.-M. Fang, J.-J. Feng, Ternary PtCoNi flower-like networks: one-step additive-free synthesis and highly boosted electrocatalytic performance for hydrogen evolution and oxygen reduction, *Int. J. Hydrogen Energy* 42 (2017) 25277–25284.
- Y. Liao, G. Yu, Y. Zhang, T. Guo, F. Chang, C.-J. Zhong, Composition-tunable PtCu alloy nanowires and electrocatalytic synergy for methanol oxidation reaction, *J. Phys. Chem. C* 120 (2016) 10476–10484.
- S. Lu, K. Eid, D. Ge, J. Guo, L. Wang, H. Wang, H. Gu, One-pot synthesis of PtRu nanodendrites as efficient catalysts for methanol oxidation reaction, *Nanoscale* 9 (2017) 1033–1039.
- Y. Cao, Y. Yang, Y. Shan, Z. Huang, One-pot and facile fabrication of hierarchical branched Pt-Cu nanoparticles as excellent electrocatalysts for direct methanol fuel cells, *ACS Appl. Mater. Interfaces* 8 (2016) 5998–6003.
- C. Zhang, W. Sandorf, Z. Peng, Octahedral Pt<sub>2</sub>CuNi uniform alloy nanoparticle catalyst with high activity and promising stability for oxygen reduction reaction, *ACS Catal.* 5 (2015) 2296–2300.
- K.M. El-Khatib, R.M.A. Hameed, R.S. Amin, A.E. Fetohi, Core-shell structured Cu@Pt nanoparticles as effective electrocatalyst for ethanol oxidation in alkaline medium, *Int. J. Hydrogen Energy* 42 (2017) 14680–14696.
- X.-X. Wan, D.-F. Zhang, L. Guo, Concave Pt-Cu nanocuboctahedrons with high-index facets and improved electrocatalytic performance, *CrystEngComm* 18 (2016) 3216–3222.
- L. Yang, Y. Ding, L. Chen, S. Luo, Y. Tang, C. Liu, Hierarchical reduced graphene oxide supported dealloyed platinum-copper nanoparticles for highly efficient methanol electrooxidation, *Int. J. Hydrogen Energy* 42 (2017) 6705–6712.
- F. Nosheen, Z. Zhang, G. Xiang, B. Xu, Y. Yang, F. Saleem, X. Xu, J. Zhang, X. Wang, Three-dimensional hierarchical Pt-Cu superstructures, *Nano Research* 8 (2014) 832–838.
- X. Du, S. Luo, H. Du, M. Tang, X. Huang, P.K. Shen, Monodisperse and self-assembled Pt-Cu nanoparticles as an efficient electrocatalyst for the methanol oxidation reaction, *J. Mater. Chem.* 4 (2016) 1579–1585.
- J. Zhang, H. Yang, J. Fang, S. Zou, Synthesis and oxygen reduction activity of shape-controlled Pt(3)Ni nanopolyhedra, *Nano Lett.* 10 (2010) 638–644.
- H. Wang, S. Chen, C. Wang, K. Zhang, D. Liu, Y.A. Haleem, X. Zheng, B. Ge, L. Song, Role of Ru oxidation degree for catalytic activity in bimetallic Pt/Ru nanoparticles, *J. Phys. Chem. C* 120 (2016) 6569–6576.
- S. An, Y.I. Kim, H.S. Jo, M.-W. Kim, M.W. Lee, A.L. Yarin, S.S. Yoon, Silver-decorated and palladium-coated copper-electroplated fibers derived from electrospun polymer nanofibers, *Chem. Eng. J.* 327 (2017) 336–342.
- K. Eid, H. Wang, V. Malgras, Z.A. Allothman, Y. Yamauchi, L. Wang, Facile synthesis of porous dendritic bimetallic platinum-nickel nanocrystals as efficient catalysts for the oxygen reduction reaction, *Chem. Asian J.* 11 (2016) 1388–1393.
- H. Zhang, H. Wang, J. Cao, Y. Ni, Hierarchical Cu-Ni-Pt dendrites: two-step electrodeposition and highly catalytic performances, *J. Alloy. Comp.* 698 (2017) 654–661.
- P. Zhang, X. Dai, X. Zhang, Z. Chen, Y. Yang, H. Sun, X. Wang, H. Wang, M. Wang, H. Su, D. Li, X. Li, Y. Qin, One-pot synthesis of ternary Pt-Ni-Cu nanocrystals with high catalytic performance, *Chem. Mater.* 27 (2015) 6402–6410.
- M.-X. Gong, X. Jiang, T.-Y. Xue, T.-Y. Shen, L. Xu, D.-M. Sun, Y.-W. Tang, PtCu nanodendrite-assisted synthesis of PtPdCu concave nanooctahedra for efficient electrocatalytic methanol oxidation, *Catalysis Science & Technology* 5 (2015) 5105–5109.
- W. Hong, J. Wang, E. Wang, Facile synthesis of PtCu nanowires with enhanced electrocatalytic activity, *Nano Research* 8 (2015) 2308–2316.
- N. Zhang, L. Bu, S. Guo, J. Guo, X. Huang, Screw thread-like platinum-copper nanowires bounded with high-index facets for efficient electrocatalysis, *Nano Lett.* 16 (2016) 5037–5043.
- Z. Li, R. Yu, J. Huang, Y. Shi, D. Zhang, X. Zhong, D. Wang, Y. Wu, Y. Li, Platinum-nickel frame within metal-organic framework fabricated in situ for hydrogen enrichment and molecular sieving, *Nat. Commun.* 6 (2015) 8248.
- R. Xing, R. Li, Y. Xu, B. Li, J. Liu, S. Liu, D. Luo, L. Mao, Hydrothermal-assisted homogeneous precipitation synthesis of dumbbell-like MnCO<sub>3</sub> nanostructures, *Ceram. Int.* 43 (2017) 14426–14430.
- X. Zhang, X. Liu, L. Zhang, D. Li, S. Liu, Novel porous Ag<sub>2</sub>S/ZnS composite nanospheres: fabrication and enhanced visible-light photocatalytic activities, *J. Alloy. Comp.* 655 (2016) 38–43.
- Y. Qi, T. Bian, S.I. Choi, Y. Jiang, C. Jin, M. Fu, H. Zhang, D. Yang, Kinetically controlled synthesis of Pt-Cu alloy concave nanocubes with high-index facets for methanol electro-oxidation, *Chem. Commun.* 50 (2014) 560–562.
- A.X. Yin, X.Q. Min, W. Zhu, W.C. Liu, Y.W. Zhang, C.H. Yan, Pt-Cu and Pt-Pd-Cu concave nanocubes with high-index facets and superior electrocatalytic activity, *Chemistry* 18 (2012) 777–782.
- Y. Xiong, Y. Ma, Z. Lin, Q. Xu, Y. Yan, H. Zhang, J. Wu, D. Yang, Facile synthesis of PtCu<sub>3</sub> alloy hexapods and hollow nanoframes as highly active electrocatalysts for methanol oxidation, *CrystEngComm* 18 (2016) 7823–7830.
- X. Yu, L. Li, Y. Su, W. Jia, L. Dong, D. Wang, J. Zhao, Y. Li, Platinum-Copper nanoframes: one-pot synthesis and enhanced electrocatalytic activity, *Chemistry* 22 (2016) 4960–4965.
- Y. Zhang, L. Zhao, J. Walton, Z. Liu, Z. Tang, Facile fabrication of PtPd alloyed worm-like nanoparticles for electrocatalytic reduction of oxygen, *Int. J. Hydrogen Energy* 42 (2017) 17112–17121.
- Y. Jia, Y. Jiang, J. Zhang, L. Zhang, Q. Chen, Z. Xie, L. Zheng, Unique excavated rhombic dodecahedral PtCu<sub>3</sub> alloy nanocrystals constructed with ultrathin nanosheets of high-energy {110} facets, *J. Am. Chem. Soc.* 136 (2014) 3748–3751.
- P.-p. Wang, H.-y. Li, H. Liu, P. He, B. Xu, X. Wang, Zinc sulfide nanosheet-based hybrid superlattices with tunable architectures showing enhanced photoelectrochemical properties, *Small* 11 (2015) 3909–3915.
- S. Mezzavilla, C. Baldizzone, A.-C. Swertz, N. Hodnik, E. Pizzutilo, G. Polymeros, G.P. Keeley, J. Knossalla, M. Heggen, K.J.J. Mayrhofer, F. Schüth, Structure-activity-stability relationships for space-confined Pt<sub>x</sub>Ni<sub>y</sub> nanoparticles in the oxygen reduction reaction, *ACS Catal.* 6 (2016) 8058–8068.
- A. Shafaei Douk, H. Saravani, M. Noroozifar, Novel fabrication of PdCu nanostructures decorated on graphene as excellent electrocatalyst toward ethanol oxidation, *Int. J. Hydrogen Energy* 42 (2017) 15149–15159.
- B.Y. Xia, H.B. Wu, X. Wang, X.W. Lou, One-pot synthesis of cubic PtCu<sub>3</sub> nanocages with enhanced electrocatalytic activity for the methanol oxidation reaction, *J. Am. Chem. Soc.* 134 (2012) 13934–13937.
- M. Gong, G. Fu, Y. Chen, Y. Tang, T. Lu, Autocatalysis and selective oxidative etching induced synthesis of platinum-copper bimetallic alloy nanodendrites electrocatalysts, *ACS Appl. Mater. Interfaces* 6 (2014) 7301–7308.
- S.K.X. Jiang, N. Zhang, S. Guo, X. Huang, Crystalline control of {111} bounded Pt<sub>3</sub>Cu nanocrystals: multiply-twinned Pt<sub>3</sub>Cu icosahedra with enhanced electrocatalytic properties, *ACS Nano* 7 (2015) 7634–7640.
- R. Xing, S. Liu, Facile synthesis of fluorescent porous zinc sulfide nanospheres and their application for potential drug delivery and live cell imaging, *Nanoscale* 4 (2012) 3135–3140.
- R.M. Xing, X.Y. Wang, C.L. Zhang, J.Z. Wang, Y.M. Zhang, Y. Song, Z.J. Guo, Superparamagnetic magnetite nanocrystal clusters as potential magnetic carriers for the delivery of platinum anticancer drugs, *J. Mater. Chem.* 21 (2011) 11142–11149.
- M. Heggen, M. Gocyla, L. Gan, P. Strasser, R. Dunin-Borkowski, Growth and Degradation of Advanced Octahedral Pt-alloy Nanoparticle Catalysts for Fuel Cells, (2016), pp. 800–801.
- Y. Kim, Y.W. Lee, M. Kim, S.W. Han, One-pot synthesis and electrocatalytic properties of Pd@Pt core-shell nanocrystals with tailored morphologies, *Chemistry* 20 (2014) 7901–7905.
- K. Wang, R. Sripathoorat, S. Luo, M. Tang, H. Du, P.K. Shen, Ultrathin PtCu hexapod nanocrystals with enhanced catalytic performance for electro-oxidation reactions, *J. Mater. Chem.* 4 (2016) 13425–13430.
- D.B. Huang, Q. Yuan, H.H. Wang, Z.Y. Zhou, Facile synthesis of PdPt nanoalloys with sub-2.0 nm islands as robust electrocatalysts for methanol oxidation, *Chem. Commun.* 50 (2014) 13551–13554.
- K. Eid, H. Wang, V. Malgras, Z.A. Allothman, Y. Yamauchi, L. Wang, Facile synthesis of porous dendritic bimetallic platinum-nickel nanocrystals as efficient catalysts for the oxygen reduction reaction, *Chem. Asian J.* 11 (2016) 1388–1393.
- H. Fan, M. Cheng, Z. Wang, R. Wang, Layer-controlled Pt-Ni porous nanobowls with enhanced electrocatalytic performance, *Nano Research* 10 (2016) 187–198.
- J. Wu, L. Qi, H. You, A. Gross, J. Li, H. Yang, Icosahedral platinum alloy nanocrystals with enhanced electrocatalytic activities, *J. Am. Chem. Soc.* 134 (2012) 11880–11883.
- S.B. Wang, W. Zhu, J. Ke, J. Gu, A.X. Yin, Y.W. Zhang, C.H. Yan, Porous Pt-M (M = Cu, Zn, Ni) nanoparticles as robust nanocatalysts, *Chem. Commun.* 49 (2013) 7168–7170.